01

Modeling of optical inhomogeneities in Cr^{2+}:CdSe lasers with a moving active element

© M.V. Volkov,[1,2,4] V.A. Garutkin,[1] N.G. Zakharov,[1,2] G.M. Mishcenko,[1] V.O. Ryabov,[2,3] F.A. Starikov[1,4]

[1] Russian Federal Nuclear Center All-Russian Research Institute of Experimental Physics, Sarov, Russia
[2] Lobachevsky State University of Nizhny Novgorod, Nizhny Novgorod, Russia
[3] Branch of the Lomonosov Moscow State University in Sarov, Sarov, Russia
[4] SarFTI National Research Nuclear University MEPHI, Sarov, Russia
e-mail: vitaliy.ryabov.1999@mail.ru

Received November 16, 2022
Revised January 23, 2023
Accepted January 24, 2023

The work is devoted to modeling the heating of moving active elements from CdSe and estimates emerging optical inhomogeneities. Active elements in the form of a parallelepiped are considered, which rotated in a circle perpendicular to the generation axis. As a result of calculations, it was found that the temperature distribution in the active element that occurs during the operation of the laser can be represented as the sum of two components. The first component is formed due to the balance between heat emission in the active element due to pumping and heat removal from it, which leads to the appearance of an aberration, which is the sum of „tilt“ and „defocusing“. The second component is formed directly during the passage of the pump spot through the active element, is determined only by the heat release density and is not related to the cooling method of the active element. It leads to the appearance of „Gaussian“ aberration, the amplitude of this aberration is directly proportional to the power of heat emission and inversely proportional to the frequency of rotation of the active element.

Keywords: mobile active elements, optical inhomogeneities of the refractive index, Cr^{2+}:CdSe laser.

DOI: 10.21883/TP.2023.03.55801.248-22

Introduction

Lasers based on chalcogenide crystals doped with divalent chromium ions (Cr^{2+}:ZnSe, Cr^{2+}:ZnS, Cr^{2+}:CdSe, Cr^{2+}:CdS, Cr^{2+}:CdTe, etc.) make it possible to obtain efficient generation with a tunable wavelength in the range from 2 to 3.6 μm [1]. The main problem limiting the power of all solid-state lasers is the efficient heat removal provision. In the case of laser media based on chalcogenide compounds doped with Cr ions, this problem is especially critical because of the large value of the thermooptical constant dn/dT. Therefore, strong thermal lenses arise in such active elements, which take the resonator out of the stability region. As a consequence — the power obtained in traditional laser schemes is low. For example, the average output power of Cr^{2+}:CdSe lasers is limited by ~ 2 W [2].

To further increase the generation power in the cw mode while maintaining a satisfactory divergence of laser radiation, it is necessary to minimize the effect of the thermal lens. For this purpose, circuits with a movable active element can be used; here the decrease in the heating of the active medium occurs due to its mechanical removal from the pumping and generation region. The use of circuits with movable active element allows heat to be „smeared“ over a larger volume and to carry out heat exchange over a rather large area of the active element. The first implementation of this approach was, apparently, the paper [3], in which a neodymium glass slab moved. An average output power of about 40 W was obtained with repetitively pulsed lamp pumping. The development of this direction led to the implementation of continuous generation with rotating active elements made of crystals [4,5].

In the paper [4] the active element made of Cr^{2+}:ZnSe crystal in the form of a ring was used, it was mounted on two cooling flanges. With the help of a DC motor, the active element was rotated. Continuous generation with a peak power of 140 W is implemented.

In the paper [5] a parallelepiped-shaped Cr^{2+}:CdSe crystal was used as active element, it moved perpendicular to the resonator axis at a speed of 28 m/s. Note that the active element was grown from the vapor phase using the technology described in [6]. In the time interval when the pump beam passes through the active element, generation with peak power of 20 W is obtained.

Optical inhomogeneities of the refractive index in the active element play an important role, since they determine the beam divergence and the limit power of the laser generation with a good beam quality. Obviously, the optical inhomogeneities of the refractive index in the mobile active

element can differ significantly from the inhomogeneities that arise in a stationary element.

The purpose of this paper is to numerically study optical inhomogeneities that arise in mobile active elements of Cr^{2+}:CdSe crystal.

1. Mathematical statement of the problem

The active element of Cr^{2+}:CdSe crystal was a parallelepiped fixed on the side surface of a rotating disk (Fig. 1). Fig. 1 also shows a round pump spot; the dashed line shows its trajectory along the active element.

The active element movement occurred in XOY plane due to its continuous rotation along a circle of radius R with an rotational speed Ω, i.e. a statement similar to [4] was considered. If the side surface of the disk is completely filled with active elements, then continuous generation can be realized. The pumping radiation is directed parallel to the axis Z. The gradient of heat release in the active element along the axis Z will depend on the change in the caustic of the pumping radiation. Since the dimensions of the active element are, as a rule, much smaller than the length of the resonator, we take as an approximation in the calculations the absence of temperature gradients along the axis Z.

To solve the problem of heating the rotating active element, a two-dimensional non-stationary heat conduction equation was solved [7]:

$$\frac{\partial T}{\partial t} = \chi\left(\frac{\partial^2 T}{\partial x^2} + \frac{\partial^2 T}{\partial y^2}\right) + F(x,y,t) - \frac{2\phi_{air}(T - T_{air})}{c_p \rho L_z}, \tag{1}$$

where χ — thermal diffusion coefficient of the crystal, $F(x,y,t)$ — function of heat release source, ϕ_{air} — coefficient of heat exchange of the active element with the environment at temperature T_{air}, L_z — length of the active element, c_p — specific-heat capacity of the active element, ρ — density of the active element. The heat-transfer equation was solved until the moment when the temperature distribution stops to change, followed by the pump spot passage through the active element.

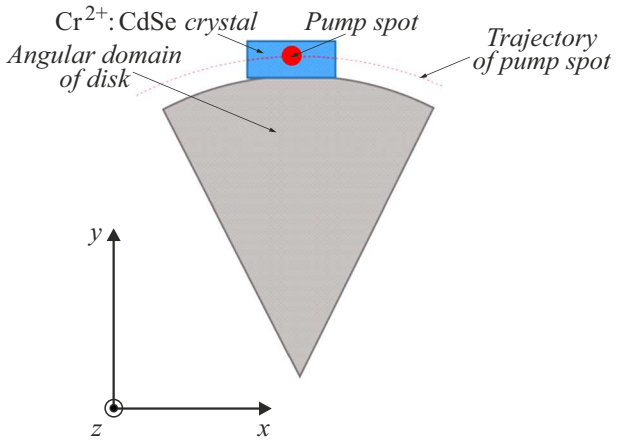

Figure 1. Geometry of the problem.

To reduce the calculation time, the problem of thermal conductivity of the mobile active element was divided into two parts: stationary and non-stationary. In the first part, the heat release is „smeared“ over the pump beam trajectory, and the stationary temperature distribution of the active element is found. The heat release function of the stationary source has the following form:

$$F(r) = \frac{P}{(c_p \rho V_{st})} \cdot \exp\left[\frac{(-2(r-R)^2)}{\omega_p^2}\right], \tag{2}$$

where $r = \sqrt{(x^2 + y^2)}$, P — heat release power in active element, R — pump spot trajectory radius, ω_p — radius of the pump spot, V_{st} — normalized volume of stationary heat source. It can be defined as

$$V_{st} = \sqrt{2\pi^3}\omega_p R L_z. \tag{3}$$

The obtained temperature field is used as the initial condition for the non-stationary part, where the pump spot acts as a source of heat release. The heat release function of the non-stationary source has the following form:

$$F(x,y,t) = \frac{P}{c_p \rho V_{ns}} \times \exp\left[\frac{-2((x - x_0(t))^2 + (y - y_0(t))^2)}{\omega_p^2}\right], \tag{4}$$

where V_{ns} — normalized volume of non-stationary source of heat release, determined by the equation

$$V_{ns} = \frac{\pi\omega_p^2}{2} L_z. \tag{5}$$

As noted above, in the calculations the active element rotates along a circle with radius R with rotational speed Ω. In this case, the coordinates of the pump spot on the active element can be determined as follows:

$$x_0(t) = R\cos(\Omega t), \tag{6}$$

$$y_0(t) = R\sin(\Omega t). \tag{7}$$

The method used for solving the problem of thermal conductivity of the mobile active element, as shown by the control comparison, describes the results of an honest solution of a non-stationary problem with good accuracy. The difference between the results is less than one tenth of a percent, but the calculation time is by an order of magnitude less.

As noted above, the active element is fixed on the periphery of the rotating disk. On the lower (closest to the center of rotation) wall of the crystal the heat exchange with thermal paste was assumed due to thermal conductivity. Therefore, the boundary condition on the lower wall of the crystal has the following form:

$$-\lambda_T \left(\frac{\partial T}{\partial y}\right)_1 = -\lambda_{AE} \left(\frac{\partial T}{\partial y}\right)_2, \tag{8}$$

Table 1. Numeric values of constants used in calculations

Parameter	Value
Crystal dimensions Cr^{2+}:ZnSe $L_x \times L_y \times L_z$	$4.5 \times 2.5 \times 4.5$ mm
Specific heat capacity of crystal Cr^{2+}:ZnSe	0.255 J/(g·K) [4]
Thermal conductivity coefficient of crystal Cr^{2+}:ZnSe	0.069 W/(cm·K) [5]
Thermooptical constant dn/dT for crystal Cr^{2+}:ZnSe	10^{-4} K^{-1} [2]
Thermal conductivity coefficient of thermal paste λT	1 W/mK
Air temperature T_{air}	22°C
Kinematic viscosity of air ν_{air}	$1.6 \cdot 10^{-5}$ m^2/s [9]
Thermal conductivity of air λ_{air}	$26.2 \cdot 10^{-3}$ W/mK [9]
Thermal expansion coefficient β_{air}	$3.67 \cdot 10^{-3}$ K^{-1} [10]
Laser radiation wavelength λ	2.8 mm
Pump spot radius ω_p	0.24 mm
Pump spot trajectory radius R	72.25 mm

where λ_T — heat conductivity coefficient of the thermal paste, λ_{AE} — heat conductivity coefficient of the active element.

On the remaining walls of the active element the convective heat exchange with air was implemented with the boundary condition:

$$\phi_{air}(T - T_{air}) = -\lambda_{AE}\left(\frac{\partial T}{\partial n}\right). \tag{9}$$

The formula for calculating the coefficient of heat exchange with air can be estimated from the formula for rotating disk [8], where we take the radius of the pump spot trajectory R as the radius of the disk:

$$\varphi_{air} = Nu\frac{\lambda_{air}}{R}, \tag{10}$$

where λ_{air} — thermal conductivity coefficient of air. The Nusselt number Nu — is a dependent parameter and is determined through the ratio of other dimensionless parameters:

$$Nu = 0.4(\mathrm{Re}^2 + Gr)^{1/4}, \tag{11}$$

where Re — Reynolds number, Gr — Grashof number. To find the Reynolds number, we used the ratio

$$\mathrm{Re} = \frac{\Omega R^2}{\nu_{air}}, \tag{12}$$

where Ω — rotational speed, ν_{air} — kinematic viscosity of air.

The Grashof number was determined according to the following expression:

$$Gr = \frac{g\beta_{air}R^3\pi^{3/2}\Delta T}{\nu_{air}^2}, \tag{13}$$

where g — gravity acceleration, β_{air} — volume expansion coefficient, ΔT — temperature difference between active element and air.

In formula (11) the Grashof number is responsible for natural convection, and in the case of high rotation rates and small temperature drops ΔT, it can be ignored when calculating the heat transfer coefficient.

The change in the beam phase $\Delta\varphi(x, y)$ after passing through the active medium L_z long with temperature inhomogeneity is determined according to the following formula:

$$\Delta\varphi(x, y) = k_0 L_z \frac{dn}{dT}T(x, y), \tag{14}$$

where $k_0 = 2\pi/\lambda$ — wave number, λ — wavelength of laser radiation.

Table 1 contains numeric values of constants used in calculations.

2. Calculation results and discussion

Let us proceed to the discussion of the results of numerical simulation. Fig. 2 shows the characteristic distribution of temperature drop $\Delta T(x, y)$ between the active element and the environment when the pump beam is outside active element and in its center. In this calculation the heat release power is $P = 40$ W, the rotation frequency of the active element is $\Omega = 100$ Hz.

For a more detailed analysis of optical inhomogeneities, let us consider the cross section of the temperature distribution along the axis y at $x = 2.25$ mm, when the pump beam is located outside the active element and at its center. These cross-sections are shown in Fig. 3.

As can be seen from Fig. 3, the temperature profiles arising in rotating active element directly in the region of the pump spot can be represented as a sum of two components. The first component is formed due to the balance between heat release in the active region and heat removal (curve *1* in Fig. 3, *a*). As can be seen from the graphs presented, this component does not change during the pump spot passage through the active element, i.e. has a regular nature. The second component is irregular, it is related to the active element heating directly during the pump spot passage (Fig. 3, *b*). Along the vertical axis the irregular component has a Gaussian profile that coincides in width with the width of the pump spot.

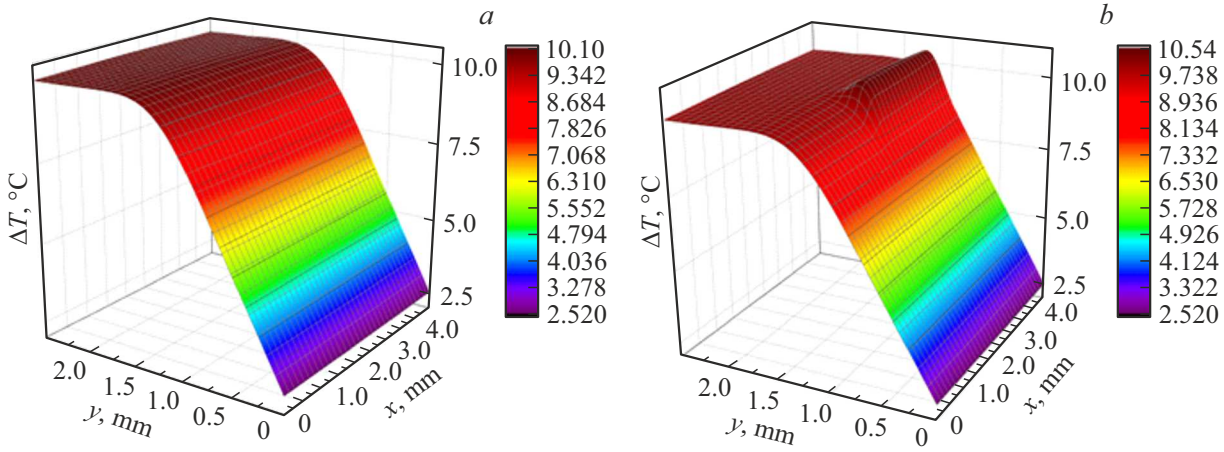

Figure 2. Distribution of temperature drop between the active element and the environment when the pump beam is outside active element (a) and in its center (b).

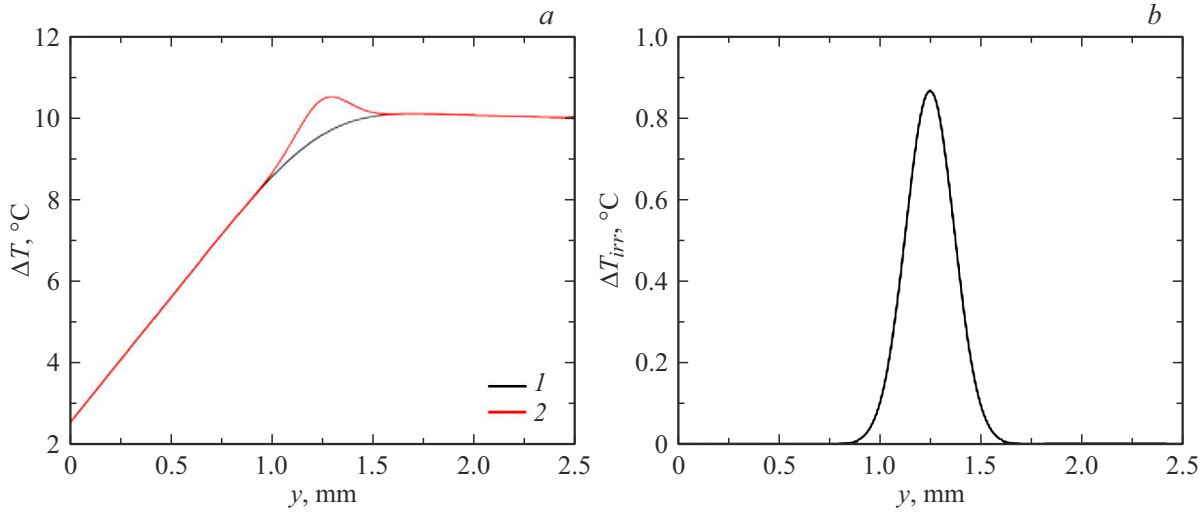

Figure 3. Cross section of temperature drop distribution along axis y at $x = 2.25$ mm (a) when the pump beam is outside the active element (1) and at its center (2), and their difference (b).

Let us first consider the optical inhomogeneity, which is formed due to the regular component of the temperature profile in the active element (curve *1* in Fig. 3, *a*).

We approximate the phase distortions by the parabolic dependence

$$\Delta\varphi(y) = Ay^2 + By + C = \frac{k}{2F_T}y^2 + k\alpha y + C, \qquad (15)$$

where F_T is the focus of the thermal lens, α is the tilt angle of the wave front. The coefficient $A = \frac{k}{2F_T}$ is responsible for abberation of „defocusing“ type, $B = k\alpha$ — for „tilt“ along the axis y.

Fig. 4 shows the profile of regular phase distortions along the axis y, its approximation by parabola, and the corresponding abberations of „defocusing“ and „tilt“ types. The characteristic size of the main mode in the experiment is — 200–400 μm, so the approximation was carried out in the range of y values from 0.75 to 1.75 mm.

Thus, the regular component of the temperature profile in the active element leads to „tilt“ and „defocusing“ aberrations. The tilt α and focus of the thermal lens F_T can be estimated from expression (15). Note that to compensate for aberrations of „tilt“ type a retroreflector of the „cat's eye“ type can be used in the experiment. For this reason, it will not play a significant role in the divergence of the laser beam. On the contrary, the size of the thermal lens is extremely important. A strong thermal lens can cause the resonant cavity to go out of the stability region and, consequently, to degrade the beam quality. When choosing the type of the resonator, this effect should be taken into account. For example, it is possible to use the resonator circuit, which considers the optical power of the resulting lens. As a rule, such circuits are developed for the given resonator type and pumping radiation power, and they operate in a narrow range of laser system parameters, see, for example, [11–13].

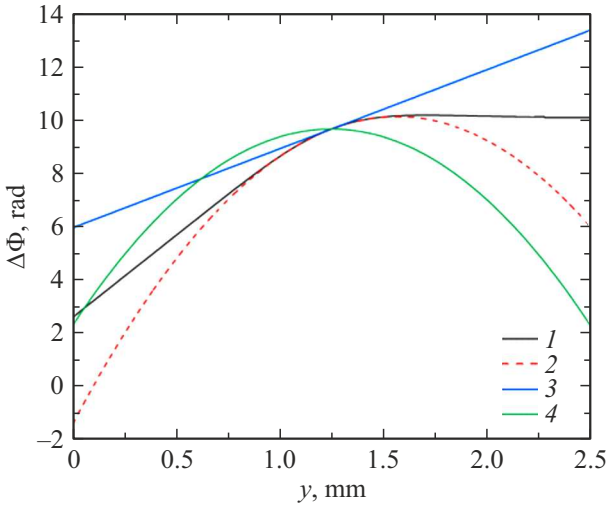

Figure 4. Profile of regular phase distortions along the axis y (*1*), its approximation (*2*) as the sum of aberrations „slope“ (*3*) and „defocusing“ (*4*).

Fig. 5 shows the results of calculations of the wavefront tilt slope α and the thermal lens focus F_T for various values of the active element rotation frequency. The heat release power in this series of calculations is — 40 W, which corresponds to the laser generation level ~ 120 W [14].

As can be seen from the results presented in Fig. 5, the tilt of wavefront weakly depends on the rotation frequency of the active element. The weak dependence of the wavefront tilt on the rotation frequency is associated with a slight increase in the coefficient of heat exchange with the environment, and, as a result, a slight increase in the heat flux leaving through the upper surface of the active element.

The focus of the thermal lens, in contrast to the tilt, significantly depends on the rotation frequency: as the frequency increases from 50 to 200 Hz, the focus of the thermal lens decreases from 70 to 50 cm. The characteristic distance L_T, over which the temperature wave propagates during the active element revolution, can be found by the formula

$$L_T = \sqrt{4\pi\chi\frac{1}{\Omega}}. \qquad (16)$$

For the frequency $\Omega = 100$ Hz the value is $L_T \approx 0.73$ mm, which is smaller than the considered crystal dimensions. Since the characteristic distance over which the temperature spreads in the active element during revolution decreases with increase in the rotation frequency of the active element, then during one revolution the heat is „smeared“ over a smaller volume of the active element. As a result, the temperature gradients in the directions from the lower and upper walls to the pumping region increase, and a stronger thermal lens is formed. Note that the choice of the rotation frequency of the active element will depend on the type of resonator and its ability to hold the thermal lens.

Fig. 6 shows wavefront tilt α and the focus of the thermal lens F_T vs. the power of heat release in the active element. The rotation frequency of the active element in this calculation is $\Omega = 100$ Hz.

The calculated dependence of the thermal lens focus is well approximated by the analytical function $F_T \sim P^{-1}$. When the pumping power is increased by 2 times, the focus of the thermal lens will also decrease by 2 times. The wavefront tilt depends linearly on the heat release power $\alpha \sim P$.

Next, we consider the change of aberrations „tilt“ and „defocusing“ when organizing an additional heat sink on the upper (most remote from the rotation axis) wall of the crystal. The range of values of heat transfer coefficients was chosen from 250 to 1500 W/m^{2}K, since the coefficient of heat exchange with water $\varphi \sim 1000$ W/m^{2}K is within this range [8]. The corresponding dependences of the focus of thermal lens and tilt on the heat transfer coefficient of the upper wall of the active element are shown in Fig. 7.

As can be seen from Fig. 7, with an increase in the coefficient of heat exchange of the upper wall with the environment, the tilt decreases due to decrease in the difference in the heat fluxes removed from the lower and upper surfaces of the active element. It is important that the value of the focus of the thermal lens practically does not change, since the total heat flux removed from the crystal walls remains constant. Accordingly, increase in the temperature gradient in the direction from the upper wall to the pumping region is „compensated“ by decrease in the temperature gradient from the lower wall to the pumping region.

Let us go to discussion of the optical inhomogeneity, which is formed due to the regular component of the temperature profile in the active element (Fig. 3, *b*). Unlike „defocusing“ and „tilt“ this optical inhomogeneity will directly affect the beam quality during laser generation. Fig. 8 shows the central sections of irregular optical inhomogeneity along the axis y.

All the presented cross-sections of the irregular optical inhomogeneity along the axis y have, like the pump beam, the Gaussian profile with width equal to the width of the pump spot. Consequently, the irregular optical inhomogeneity is determined only by the heat release density and does not depend on the rate of heat exchange with the environment.

The corresponding to Fig. 8 dependences of the value of the phase incursion $\Delta\varphi_{\max}$ at $y = 1.25$ mm on the heat release power and the rotation frequency of the active element are shown in Fig. 9.

Dependence of maxima of phase incursion $\Delta\varphi_{\max}$ of irregular optical inhomogeneity on heat release power and rotation frequency of the active element has the following form:

$$\Delta\varphi_{\max} \sim \frac{P}{\Omega}. \qquad (17)$$

Thus, in the experiment with increase in the pumping radiation power by 2 times (which corresponds to increase

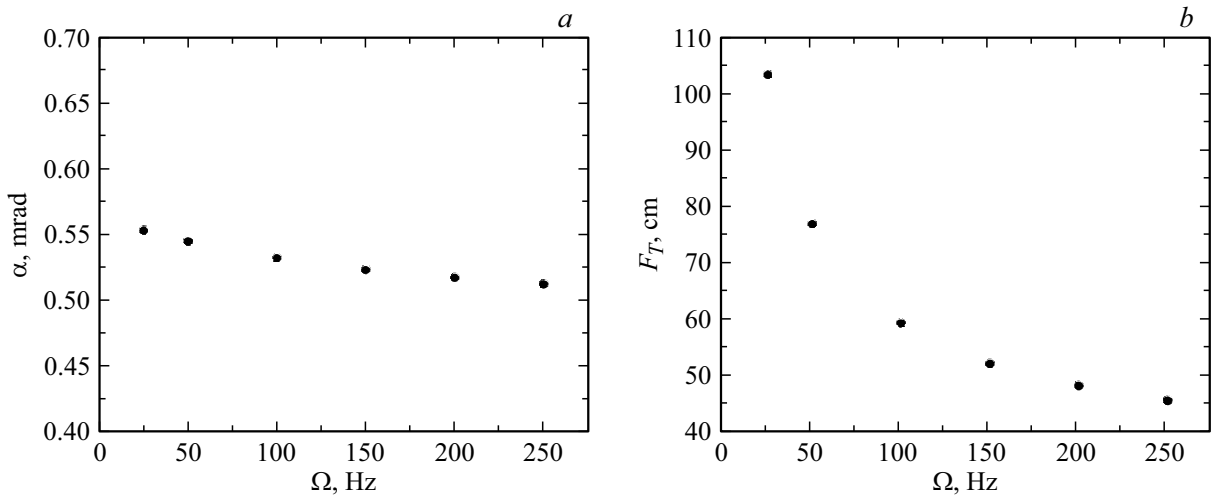

Figure 5. Tilt (a) and focus of the thermal lens (b) vs. speed of the active element.

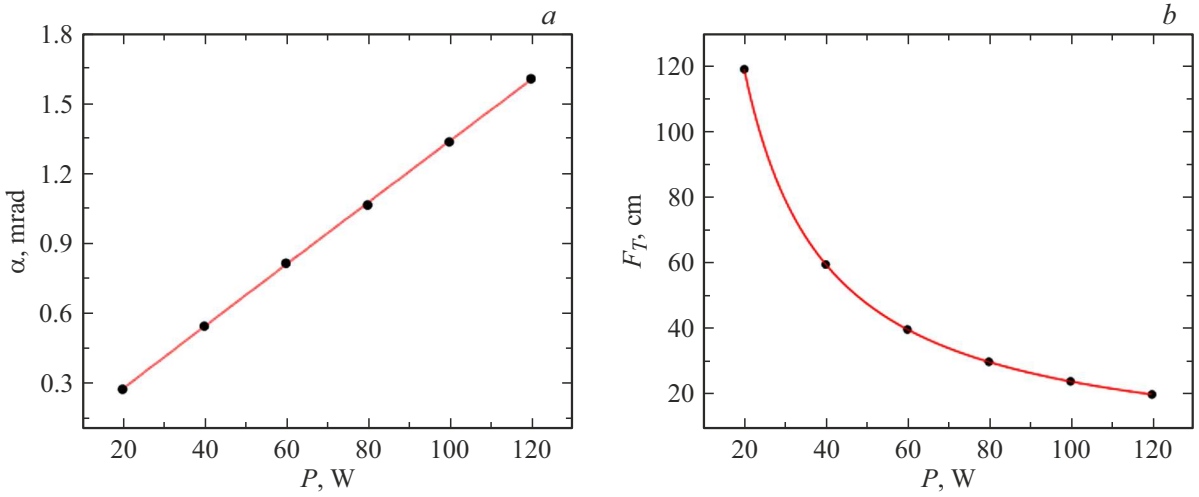

Figure 6. Wavefront tilt (a) and the focus of the thermal lens (b) vs. the power of heat release in the active element.

Table 2. Thermooptical and spectroscopic properties of crystals

Laser crystal	ZnSe	CdSe	CdTe
Heat capacity θ, J/(g·K)	0.34 [1] 0.339 [4.5]	0.255 [4] 0.258 [5]	0.205 [4] 0.21 [5]
Thermal conductivity coefficient q, W/(cm·K)	0.13 [5]	0.062(‖a) [5] 0.069(‖c) [5]	0.0585 [4] 0.063 [5]
Thermooptical constant dn/dT, $\cdot 10^{-6}\,\mathrm{K}^{-1}$	63.4 [1] 59.7–52 [5]	100 [1]	147–98.2 [5] 100 [14]

in the heat release power by ~ 2 times), in order to maintain the laser beam divergence at the same level it is also necessary to increase the rotation frequency of the active element by 2 times also.

Table 2 presents the thermooptical properties of Cr^{2+}:ZnSe and Cr^{2+}:CdTe crystals. For comparison, the data for Cr^{2+}:CdSe are also given there. Among chalcogenides doped with Cr^{2+} ions these crystals have high amplification cross-sections in the spectral range from 2 to 3.6 μm.

As can be seen from the Table, the thermooptical properties of the CdTe and CdSe crystals are numerically very close, and ZnSe crystal has better properties. The thermal conductivity of ZnSe is by more than two times higher, and dn/dT is approximately by 1.6 times lower. It

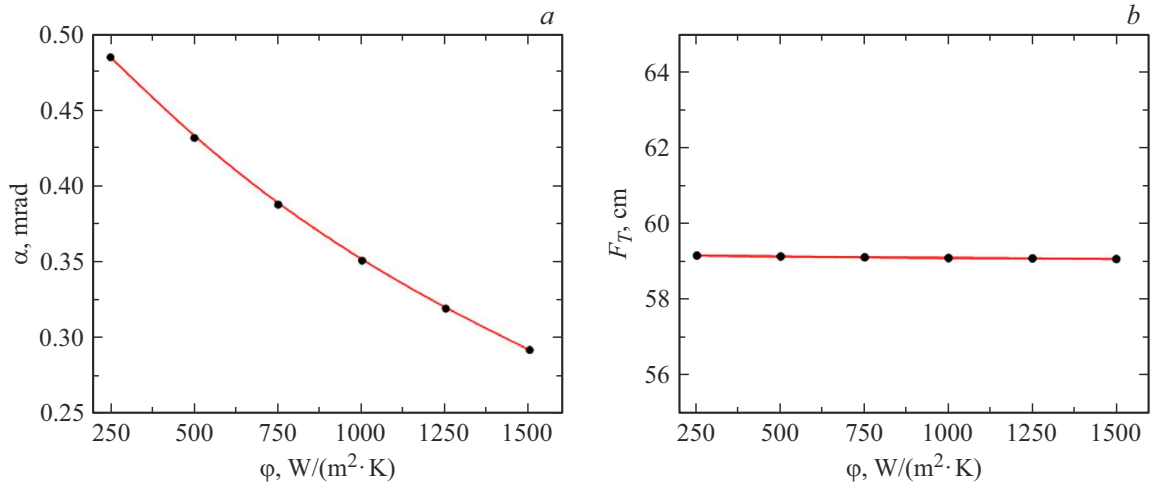

Figure 7. Tilt (a) and focus of the thermal lens (b) vs. coefficient of heat exchange between the upper wall of the active element and the environment.

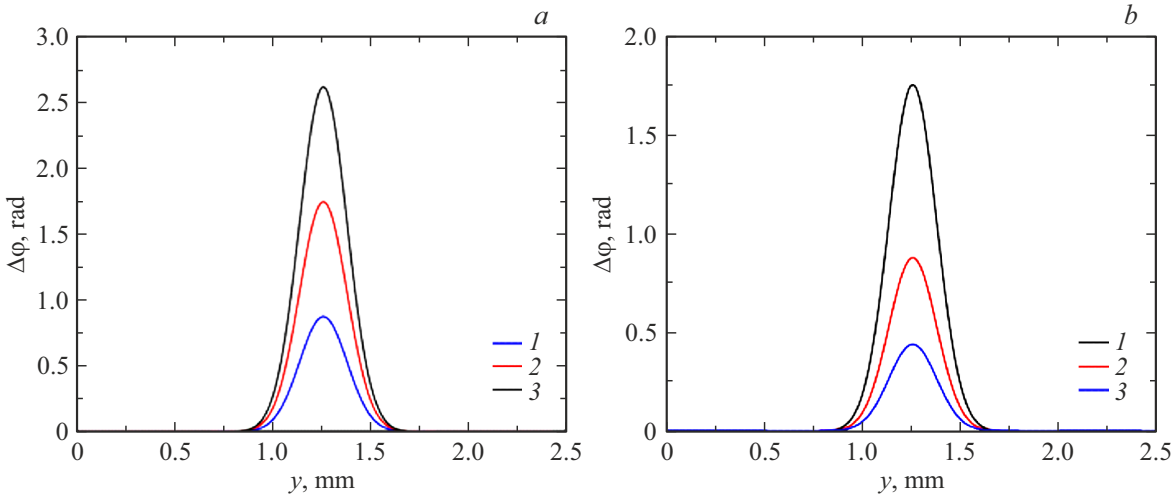

Figure 8. Central sections of irregular optical inhomogeneity along the axis y, a — for different heat release power: *1* — 40, *2* — 80, *3* — 120 W (at $\Omega = 100$ Hz); b — at different rotation frequencies of the active element: *1* — 50, *2* — 100, *3* — 200 Hz (at $P = 40$ W).

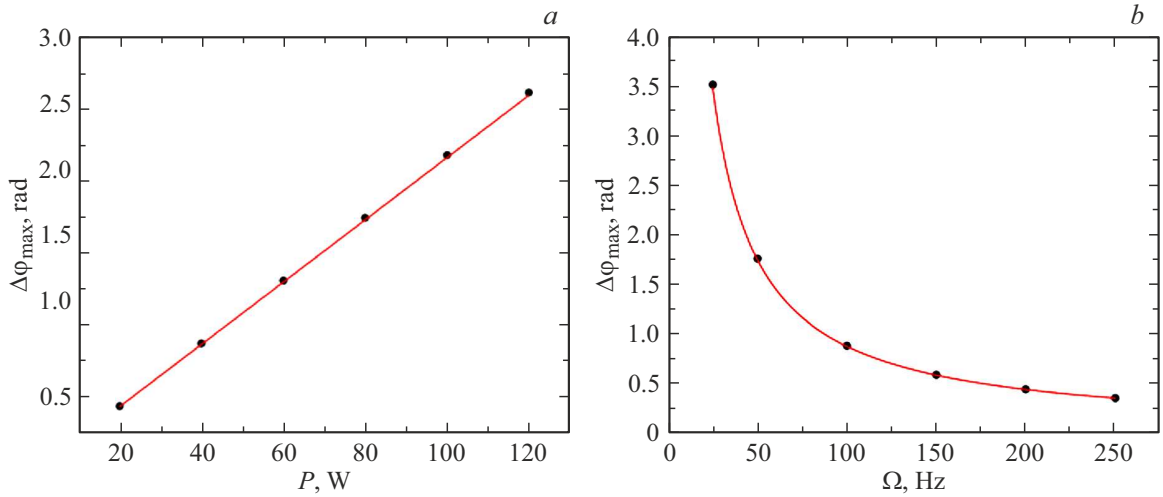

Figure 9. Maxima of phase incursion $\Delta\varphi_{max}$ of irregular optical inhomogeneity: a — vs. heat release power, b — vs. rotation frequency of the active element.

follows from this that in the experiment, other things being equal, in ZnSe crystal the required rotational frequencies of the active element are by four times lower. Also, in ZnSe crystal the thermal lens will be by ~ 4 times weaker, in other words, the limit pumping radiation power for ZnSe crystal is by ~ 4 times greater.

Conclusion

The paper is devoted to numerical modeling the heating of rotating laser active elements from Cr^{2+}:CdSe and estimates of emerging optical inhomogeneities. Active elements in the form of a parallepiped are considered, which rotated on disk perpendicular to the generation axis. It was assumed that thermal paste was applied on the lower (closest to the center of rotation) wall of the element, and convective heat exchange with air was implemented on the remaining walls.

The complete „brute“ problem of heating the rotating active element is three-dimensional and non-stationary, and its solution requires large amounts of computer memory and time. To reduce the calculation time, the problem of thermal conductivity of the rotating active element was divided into two parts: stationary and non-stationary. At the stationary stage the heat release from the pump spot is „smeared“ over the ring trajectory of the spot, and the temperature distribution in the active element is found in the first approximation, which is then used as the initial condition for the non-stationary problem with rotation. This approach, as the control comparison show, with good accuracy describes the results of „full“ calculation. The difference between the results is less than one tenth of a percent, but the calculation time is by an order of magnitude less.

As a result of calculations, it is shown that the distribution of temperature (and, accordingly, the refraction index) in the active element, that occurs during the laser operation, can be conditionally divided into two components.

The first component is formed due to the balance between heat emission and heat removal from the active element, which leads to the appearance of aberration, which is the sum of „tilt“ and „defocusing“. The amplitude of these aberrations depends on the pumping power and the heat exchange coefficient of the active element with the environment. In the case of a plane-spherical ’resonator in the experiment the aberration „tilt„ is compensated by turning a blind mirror and does not affect the quality of the laser beam. Aberration „defocusing“ can lead to a deterioration in the beam quality, so its value should be taken into account when choosing the type of resonator.

The second component of the temperature profile is formed directly during the passage of the pump spot through the active element and has the same spatial distribution as the pump beam. It depends only on the heat release density and is not related to the cooling method of the active element. The amplitude of the corresponding aberration is directly proportional to the heat release power and inversely proportional to the rotation rate of the active element. Note that this aberration will directly degrade the quality of the laser beam; to reduce its effect it is necessary to increase the rotation frequency of the active element.

Funding

This paper was supported by the national project „Science and Universities“ (project FSWR-2021-012) funded by Federal Budget subsidy for financial support of the state task for the implementation of research work.

Conflict of interest

The authors declare that they have no conflict of interest.

References

[1] S. Mirov, V. Fedorov, I. Moskalev, D. Martyshkin, Ch. Kimet. Laser Photon Rev., **4** (1), 21 (2010). http://dx.doi.org/10.1002/lpor.200810076
[2] M.K. Tarabrin, D.V. Ustinov, S.M. Tomilov, V.A. Lazarev, V.E. Karasik, V.I. Kozlovsky, Yu.V. Korostelin, Yan K. Skasyrsky, M.P. Frolov. Opt. Express, **27** (9), 12090 (2019). https://doi.org/10.1364/OE.27.012090
[3] S. Basu, R. Byer. Opt. Lett., **11** (10), 617 (1986). DOI:10.1364/OL.11.000617
[4] I. Moskalev, S. Mirov, M. Mirov, S. Vasilyev, V. Smolski, A. Zakrevskiy, V. Gapontsev. Opt. Express, **24** (18), 21090 (2016). https://doi.org/10.1364/OE.24.021090
[5] N.G. Zakharov, R.A. Zorin, V.I. Lazarenko, E.V. Saltykov, A.A. Lobanova, A.V. Marugin, V.A. Garyutkin, G.M. Mishchenko, M.V. Volkov, F.A. Starikov. Pisma v ZhTF,**48** (6), 16 (2022). (in Russian). https://doi.org/10.1364/OE.24.021090
[6] V.A. Akimov, V.I. Kozlovsky, Yu.V. Korostelin, A.I. Landman, Yu.P. Podmarkov, Ya.K. Skasyrsky, M.P. Frolov. Kvant. elektron., **38** (3), 205 (2008). (in Russian).
[7] A.N. Tikhonov, A.A. Samarsky. *Uravneniya matematicheskoy fiziki* (Nauka, M., 2004) (in Russian)
[8] H. Wong. *Osnovnye formuly i dannye po teploobmenu dlya inzhenerov*. Spravochnik (Atomizdat, M., 1979) (in Russian).
[9] D.R. Lide. *Handbook of Chemistry and Physics, 84th Ed.* (CRC Press, 2003-2004)
[10] I.K. Kikoin, (red.) *Tablitsa fizicheskikh velichin*. Spravochnik (Atomizdat, M., 1976) (in Russian)
[11] W. Koechner. *Solid-State Laser Engineering* (Springer, 2013), v. 1. DOI:10.1007/0-387-29338-8
[12] A. Bereczki, N. Ursus. Opt. Laser Technol., **96**, 271 (2017).
[13] M. Harlander, A. Heinrich, C. Hagen, B. Nussbaumer. Proc. SPIE, **8959**, 895908-1 (2014).
[14] U. Hommerich, I.K. Jones, Ei Ei Nyein, S.B. Trivedi. J. Crystal Growth, **287**, 450 (2006).

Translated by I.Mazurov